

**Assessing Land Surface Growth Efficiency Variation  
Using a Climate-calibrated Phenological Index**

Liang Liang  
Department of Geography  
University of Wisconsin-Milwaukee  
Milwaukee, WI 53211  
Phone: 414-229-2436  
Fax: 414-229-3981  
Email: lliang@uwm.edu

Mark D. Schwartz  
Department of Geography  
University of Wisconsin-Milwaukee  
Milwaukee, WI 53211  
Phone: 414-229-3740  
Fax: 414-229-3981  
Email: mds@uwm.edu

Michael A. White  
Department of Watershed Sciences  
Utah State University  
Logan, Utah 84322  
Phone: 435-797-3794  
Fax: 435-797-1871  
Email: mikew@cc.usu.edu

## **Abstract**

Spring plant phenology integrates signals from both climate variations and intrinsic physiology. Given the need to track potential climatic change impacts on phenotypic plasticity of plant functional types, it is useful to develop phenological indices that are independent of climatic influence. Remotely sensed start of season (Delayed Moving Average Start of Season, DMA SOS) and a phenological model (Spring Indices, SI) at 1 km x 1 km resolution are used to formulate a “Growth Efficiency Index” (GEI) for the conterminous US over the 13-year period 1989-2001. Multiplication relationships are used to model interactions between climate and plant physiology. Hence, GEI is calculated with a band ratioing algorithm from DMA SOS and SI as image algebra data layers. The resultant GEI varies in response to different levels of energy needed by diverse terrestrial ecosystems for spring season onset. Selected vegetation cover types from the U.S. Geological Survey National Land Cover Database (NLCD, 2001 version) are compared with GEI within delineated regions. Strong dependence ( $R^2=0.657$ ) of GEI on latitude, longitude (proximity to ocean), and altitude is typical in the eastern US, essentially the inverse of Hopkin’s Law. Trend analysis of GEI time series for major vegetation cover types does not suggest obvious inherent ecosystem changes over the study period. Climate-calibrated phenological indices have the potential to be widely applied for assessing subtle changes in internal ecosystem properties, before plasticity thresholds are surpassed and range shifts occur due to climatic warming.

## **1. Introduction**

Earth's terrestrial ecosystems are driven by solar energy according to the annual seasonal cycle. Particularly before and during spring, increasing local insolation in the atmospheric boundary layer triggers vegetation growth resumption for most mid-latitude land regions (Christopherson 2006; Miller 1981). This phenomenon (onset of spring), as addressed by phenology research, is an important indicator of global climatic change (Schwartz 1994). During the past two decades, in order to address global scale tasks, especially to complement limited conventional surface data, bioclimatic modeling and satellite imagery have been employed to reveal vegetation phenology patterns at regional to global scales (de Beurs and Henebry 2005; Justice et al. 1985; Moulin et al. 1997; Schwartz 1997; Zhang et al. 2006). These large scale patterns, appearing as spring "green waves", yield significant ecological information for global change studies (Schwartz 1994, 1998).

Externally driven by the seasonality of environmental factors, vegetation phenology (onset of spring plant growth) is likewise regulated by each biome's internal phenotypic character, which derives from plant genetics and facilitates adaptation to various climates (Woodward 1987; Zhu 1980). One crucial aspect of this physiology is that each plant community or ecosystem has a characteristic level of energy utilization for subsistence, which is the basis for maintaining vitality and fulfilling healthy life cycles (Budyko 1974; Monteith 1975). From the perspective of continental scale monitoring, if a standard method can be developed to detect the varying degrees of energy absorptivity, then inherent differences/changes of biome physiology can be examined in terms of their energy consumption scheme, which actually is a key criterion for classifying different biomes or plant functional types under external climatic

forcing (Box 1996; Prentice et al. 1992). Such an assessment could be quite useful in separating the thermal demand “nature” of land vegetation from environmental fluctuations.

Studies of spring plant phenology have extensively confirmed a global warming trend for the Northern Hemisphere (Cleland et al. 2007; Menzel et al. 2006; Schwartz et al. 2006). Given the extent of the warming, it is likely that modifications to surface energy budgets are also occurring, which may have implications for each biome’s energy utilization scheme, including the potential for changes to occur within the system, before and during any possible range shift (Diaz and Cabido 1997; Huntley 1991; Malcolm et al. 2002; Overpeck et al. 1991; Peñelas and Boada 2003; Potvin and Tousignant 1996). Hence, it would be extremely useful to have metrics available to gauge these inherent changes within vegetation cover types and their potential impacts on species distribution. This paper describes an approach to develop such a measure: a Growth Efficiency Index (GEI), based on satellite-derived and bioclimatic-modeled continental-scale vegetation phenology.

## **2. Data**

### **2.1 Remotely Sensed Continental-Scale Phenology: Start of Season (SOS)**

Most remotely sensed phenological studies rely on vegetation indices (VI) and satellite sensors that provide medium spatial resolution and high temporal resolution capabilities. These data include generic Normalized Difference Vegetation Index (NDVI) data collected by Advanced Very High Resolution Radiometers (AVHRR) onboard NOAA series satellites since the 1980s (Eidenshink 1992; Goward et al. 1985; Rouse Jr et al. 1974; Tarpley 1991); and more recently NDVI and Enhanced Vegetation Index (EVI) data from the Moderate Resolution Imaging Spectroradiometers (MODIS) on board NASA Terra (EOS AM) and Aqua (EOS PM) satellites since 2000 (Huete et al. 2002; Jensen 2000; Justice et al. 1998). Determining start of

season (SOS) via VI curves has been accomplished with methods ranging from simple threshold assignment to relatively sophisticated curvature analysis (Fischer 1994; Lloyd 1990; Markon et al. 1995; Reed et al. 1994; White et al. 1997; Zhang et al. 2003).

The satellite phenology data used for this project is the Delayed Moving Average (DMA) SOS time series produced for the conterminous US over 1989 to 2001, based on 1 km resolution bi-weekly AVHRR NDVI maximum composite imagery (Reed et al. 1994). The DMA SOS method basically detects temporal points of departures from a predicted trend (the moving average of NDVI values) as the onset of growing season, or SOS. The reason this SOS dataset was chosen was its availability over a relatively long time period, and its extensive cross-validation with simulated surface phenology indices (Schwartz and Reed 1999; Schwartz et al. 2002).

## **2.2 Modeled Continental-Scale Phenology: Spring Indices (SI)**

Schwartz (1997) constructed an empirical temperature-driven set of continental-scale phenological models (Spring Indices, SI) using a multiple regression approach that incorporated cloned lilac and honeysuckle phenological data across eastern North America. The output metrics include Composite Chill Date (time when plant chilling requirements are met before they actively respond to spring warmth), First Leaf Date (time of simulated first leaf event) and First Bloom Date (time of simulated first bloom event). SI models were constructed based on typical spring conditions in the eastern US where water stress is rare, so the models do not include a moisture variable. Hypothetically, SI model predictions for fragmentary regions with significant water stresses will unavoidably deviate; however, for most temperate areas, the accuracy of SI has been extensively validated (Schwartz et al. 2006). This project uses the SI First Leaf Index for the entire conterminous US calculated at 1 km resolution, excluding some regions where the

SI models cannot be calculated due to inadequate chilling accumulation (these areas are mostly in the southern US). This data set was also produced for the 1989 to 2001 time period from DAYMET weather records (<http://www.daymet.org/>) in order to compare with DMA SOS over the same temporal span.

### **3. Methodology**

#### **3.1 Rationale of GEI**

Plant phenological timing is determined by both internal and external drivers. Internally, plant phenology varies by individual, population, community, and landscape (ecosystem patch, comparable in size with medium-resolution satellite pixels) mainly due to the innate genetic differences of plants and heterogeneity of vegetation cover at different spatial scales of observation. Externally, plant phenology is driven by the factors which include weather and climate, as well as other secondary environmental factors like underlying soil conditions (Badeck et al. 2004; Barbour et al. 1987; Fisher et al. 2006; Leopold 1951; Rosenberg 1983; Schaber 2002). At the continental-scale of interest in this study, SOS basically represents the observed integrated signals of spring phenology from the combined influence of both internal vegetation characteristics and external climatic drivers. Meanwhile, SI is a function of chilling/heat unit accumulations, and therefore works as a surrogate of external energy conditions adjusted to the needs of plants. The premise of this project is that if climate variability can be separated from the integrated phenological signals, the remaining portion would be able to reveal the inherent nature of vegetation cover in terms of their different energy consumption needs. Consequently the proposed Growth Efficiency Index (GEI) is generated by standardizing SOS (integrated signal) with SI (climate condition). The relationship between the three measures is shown in Figure 1.

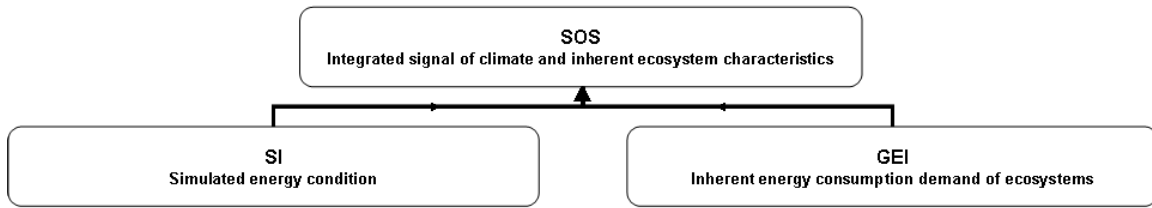


**Figure 1: Relationships among start of season (SOS), spring indices (SI) and growth efficiency index (GEI).**

### 3.2 Derivation of GEI

Given that the relationship between climate and plant genetics is interactive rather than additional, GEI is calculated by using a ratioing algorithm. SOS is divided by SI, in order to standardize land surface phenology with climatic conditions.

$$GEI = a + b \left( \frac{SOS}{SI} \right)$$

**Equation 1: Algorithm of growth efficiency index (GEI).**

Notes:

- 1). GEI is the linear transformation of the ratio between SOS and SI
- 2). Units of all the variables are day of year (DOY)
- 3). a and b are arbitrary constants for scaling GEI to reasonable DOY ranges; they reflect hypothetical standard climate conditions across the entire study area

Image processing tasks were done with ERDAS IMAGINE 9.1 software. Iterative processes were used to determine the appropriate constants, which are data specific and needed to scale GEI values into a typical DOY range (numbers from 0 to 255 are used since the DOY of spring onset should range from spring to summer). Such scaling provides the GEI values with phenological meaning in relation to a simulated standard climate. Thus, the fitting parameters (a and b) represent a hypothesized climate that is uniformly applied to the entire study area. The resultant GEI values showing spatial variations similar to the typical range of SI onset times across the contiguous US. The biophysical meaning of this new index is intrinsically a SOS which has been standardized and detached from climate variations, with derived GEI showing

inherent efficiency variations of vegetation growth through the timing (in DOY) of the simulated spring onset.

## 4. Results and Analyses

### 4.1 GEI Map for the Conterminous US

GEI maps for the conterminous US were first produced for individual years respectively. Then a principle component analysis was done over the entire 13 year time period to extract consistent spatial distribution patterns of GEI. This resultant GEI map should reduce data/model noise and interannual weather fluctuations (which may have not been entirely removed by standardization), and thus better represent differing innate energy consumption regimes across the country (Figure 2).

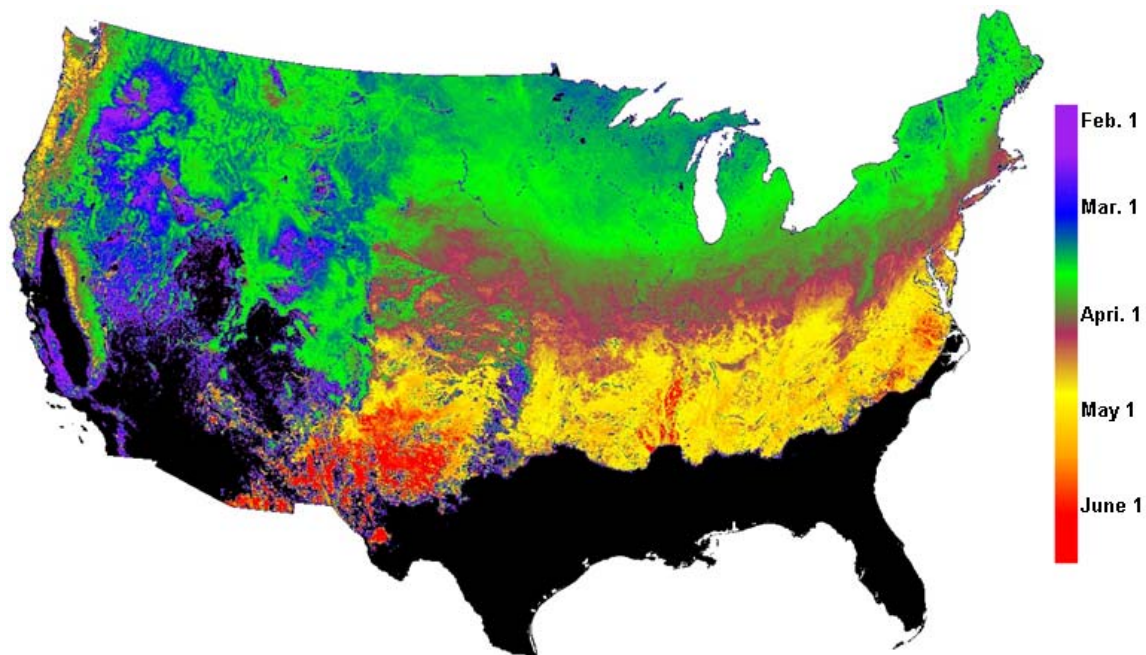


**Figure 2: Growth Efficiency Index (GEI) map for the conterminous US, produced from 13-year (1989-2001) start of season (SOS) and first leaf spring indices (SI) data, integrated with principle component analysis (partial areas <in black> omitted due to model inapplicability). Earlier GEI dates correspond to lower energy demands for spring season onset.**

The derived GEI in most parts of the conterminous US follow apparent spatial transitional patterns with latitude, elevation and proximity to ocean. It generally tracks Hopkins'

bioclimatic law, but with an inverse relationship (Hopkins 1938). GEI dates are earlier in higher latitude or higher altitude areas, indicating less energy is needed by plants in colder regions to push through winter-spring transitions. In the east, GEI dates are delayed when the location of interest is closer to the east coast due to the marine effects. Distribution of GEI also approximates the spatial configuration of known major climatic regions (Christopherson 2006).

Latitude, longitude and GTOPO30 1 km resolution DEM data from the U.S. Geological Survey (USGS) EROS Data Center (<http://edc.usgs.gov/>) were used to quantify their predictive power for GEI variations. According to visually distinguishable GEI spatial arrangement patterns, four specific regions (East, Middle, Mountain and Pacific) were arbitrarily delineated. An evaluation of the linear relationship between the GEI and geographic locations (latitude, longitude and altitude) of these four regional groups was measured using Pearson's correlation. The analysis using Pearson's correlation indicated significant correlations ( $P < 0.001$  for all cases) for all pairs of variables, with varying strengths of the correlation coefficients (Table 1).

**Table 1: Pearson correlations between GEI and geographic locations  
( $P < 0.001$  for all cases)**

GEI by Regions	Statistics	Latitude	Longitude	Altitude
Eastern Region	Pearson Correlation	<b>-0.788</b>	<b>-0.278</b>	<b>-0.119</b>
	Sig. (2-tailed)	0.000	0.000	0.000
Middle Region	Pearson Correlation	<b>-0.710</b>	<b>-0.032</b>	<b>-0.104</b>
	Sig. (2-tailed)	0.000	0.000	0.000
Mountain Region	Pearson Correlation	<b>-0.145</b>	<b>0.277</b>	<b>0.104</b>
	Sig. (2-tailed)	0.000	0.000	0.000
Pacific Region	Pearson Correlation	<b>0.111</b>	<b>-0.386</b>	<b>0.172</b>
	Sig. (2-tailed)	0.000	0.000	0.000

Fitted multiple linear regression models indicated stronger linear relationships ( $R^2=0.657$ ,  $P < 0.001$ , East; 0.513,  $P < 0.001$ , Middle) in the east and middle US. In the western Mountains and Pacific Coastal areas, linear relationships were weaker ( $R^2=0.091$ ,  $P < 0.001$ , Mountain; 0.184,  $P < 0.001$ , Pacific). Specifically in the eastern US, according to the bioclimatic law, SOS is delayed approximately four days with 1 degree of latitudinal increment (northward), or 5 degree

of longitude decrease (westward), or 122 meter increase of elevation (upward). Derived GEI for the east region coincides with this relationship in a reversed direction, showing a strong adaptation of vegetation to their respective climates (Table 2). The role of elevation in determining spring onset in both models is not as clear as it is for latitude and longitude. This discrepancy may come from the inherent accuracy and precision of SI model and SOS data used to derive the GEI index, as well as of the GTOPO elevation data.

**Table 2: Comparison of GEI and Hopkins Bioclimatic Law in the eastern US**

	SOS Delay (day)	Latitude Northward (degree)	Longitude Westward (degree)	Elevation Upward (meter)
Derived GEI	- 4	0.8	5	364
Bioclimatic Law	4	1	5	122

## **4.2 Comparison of GEI with Vegetation Types**

### **4.2.1 Visual Comparison across the Conterminous US**

GEI is a new land cover characterization scheme which addresses the different levels of energy demand of vegetated land surface across the continent. In order to better visually compare GEI and identify conventional land cover types, continuous GEI data are generalized into seven thematic Energy Demand Levels (EDLs) using an unsupervised classification approach (Figure 3).

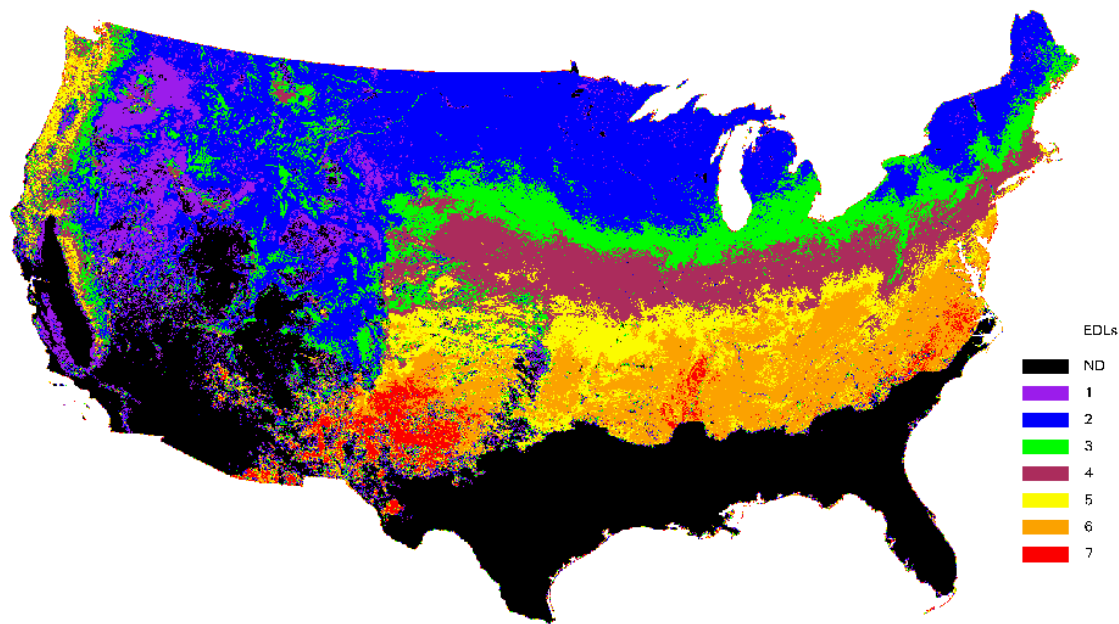


**Figure 3: Energy Demand Levels (EDLs) generalized from the growth efficiency index (GEI) map for the conterminous US. ND= “No Data”. Energy demands go from low (1, purple) through high (7, red).**

USGS National Land-cover Database (NLCD) 2001 version provides a high accuracy vegetation cover dataset (Homer et al. 2004). NLCD is derived from 30 m resolution LANDSAT data and has become available for the entire US since 2006. The high resolution of NLCD provides sufficient accuracy and information base for reliable visual comparison and statistical analysis at the current scale of study. The entire NLCD map for the conterminous US is degraded to 1 km x 1 km resolution by using a majority rule filter. Detailed land cover classifications are generalized into several major classes (forests, shrub/grassland, agricultural lands, wetlands, as well as non-vegetated land covers) and then visually compared with GEI EDLs through geo-linking both images. EDLs extend across boundaries of the vegetation cover types and coincide more with the general climatic regions of the conterminous US.

East of the Rocky Mountains, EDLs of forests, shrub/grassland, and agricultural lands all respond uniformly to latitude, longitude and elevation in most locations. The direction of longitudinal effects is reversed on opposite sides of Lake Michigan, as also indicated in the previous correlation studies. Two separate regions were delineated accordingly because of this reversal. The eastern portion apparently reflects the marine influence of the Atlantic Ocean. The western portion may be affected by increasing water stress that delays the onset of spring when moving towards semiarid steppes. GEI appears to reflect the adapted inherent heat characteristics of vegetation in this climatic transition region. Forests on the Appalachian Mountains have lower EDLs compared to that of its surrounding plains due to forest physiology adapting to the relatively cooler marine west coast climate. Pseudo exceptionally high energy demand areas are found in the lower Mississippi river valley and along the east side of the Appalachian Mountains, which are areas of concentrated croplands. The reason that these high EDL signals are ascertained to be pseudo is that the phenology of crops is heavily determined by agricultural practices (mainly a function of planting time), and therefore does not reflect natural variability. In addition, the shrub/grassland cover in northwestern Texas and New Mexico appears to have locally very high EDL, which may corresponds to its hot/dry climate caused by continental tropical air masses that form over this area during the summer. The land surface phenology in this area is likely to be more water-limited; it appears to have a pseudo extraordinary high energy requirement since energy alone does not trigger photosynthesis until the minimum water requirement is met. In addition, it is very likely that C4 plants (which prefer higher temperatures and utilize water more efficiently) in this region may contribute to the high EDL signals.

The west-east belt-like distributions of EDLs are disrupted in the Rocky Mountain area where topography complicates the local climates. Some evergreen forests found on higher elevations tend to show higher energy demand than deciduous grass/shrubs found at nearby lower elevations. The contrasting physiology of these two vegetation cover types may be responsible for obscuring the correlation between GEI and elevation controlled microclimatic variations. Vegetation found along river valleys and within basins (mainly agricultural lands) appear to have higher energy demand levels than the surrounding shrub/grassland, apparently related to farming or grazing activities. Xeric shrub/grasslands in the basin and range province are mostly void of data.

Along the West Coast, EDLs appear in unique north-south oriented narrow belts along the coastline as affected by both marine and orographic effects. In Washington and Oregon the closer to the Pacific Ocean, the higher EDLs are; the higher the elevation when going eastward against mountains, the lower the EDLs are, with exceptions for agricultural lands and developed regions. Indicative meaning of EDLs in areas like California (mostly void of data) is generally obscured due to the absence of temperature driven phenology (the phenology in California primarily responds to winter moisture under Mediterranean climate) and highly managed agricultural activities.

#### **4.2.2 Quantitative comparison by regions.**

The GEI concept hypothesizes that for the same type of vegetation cover across a large area, the corresponding energy consumption regimes vary with their adapted climates. Using the detailed 1 km x 1 km NLCD map for the conterminous US, analysis of GEI correspondence with vegetation types is conducted for four delineated regions as described in section 4.1. Land cover types that occupy over 5% of the total area of each region were selected for analysis (Table 3).

**Table 3: Percentage of NLCD covers by regions.**  
(5% above marked as bold, value in %)

NLCD Classifications	East	Middle	Mountain	Pacific
11. Open Water	1.6	1.5	0.4	0.9
12. Perennial Ice/Snow	0	0	0.1	0.2
21. Developed, Open Space	4.2	2.2	0.5	1.6
22. Developed, Low Intensity	2.5	1.1	0.3	1.3
23. Developed, Medium Intensity	1.0	0.3	0.1	0.5
24. Developed, High Intensity	0.4	0.1	0	0.2
31. Barren Land (Rock/Sand/Clay)	0.3	0.1	0.9	2.2
41. Deciduous Forest	<b>42.4</b>	<b>14.2</b>	2.4	1.3
42. Evergreen Forest	<b>7.1</b>	2.5	<b>26.2</b>	<b>62.1</b>
43. Mixed Forest	<b>5.7</b>	0.8	0.2	3.5
52. Shrub/Scrub	1.3	2.4	<b>36.8</b>	<b>16.0</b>
71. Grassland / Herbaceous	1.8	<b>22.7</b>	<b>21.0</b>	4.1
81. Pasture/Hay	<b>12.3</b>	<b>9.5</b>	1.9	3.1
82. Cultivated Crops	<b>14.9</b>	<b>38.9</b>	<b>8.5</b>	1.8
90. Woody Wetlands	4.0	2.6	0.5	0.7
95. Emergent Herbaceous Wetlands	0.5	1.2	0.4	0.5

An evaluation of the linear relationship between the GEI of each major vegetation cover types and geographic locations (latitude, longitude and altitude) was measured using Pearson's correlation. The analysis using Pearson's correlation indicated significant correlations ( $P < 0.001$  for all cases) for all pairs of variables, with varying strengths of correlation coefficient (Table 4), similar to results from a previous analysis (section 4.1) but with more detail.

**Table 4: Pearson correlation of GEI  
and geographic locations by vegetation types  
(P<0.001 for all cases)**

Regions	GEI	Latitude	Longitude	Altitude
East	Deciduous	<b>-0.814</b>	<b>-0.468</b>	<b>-0.047</b>
	Evergreen	<b>-0.855</b>	<b>-0.525</b>	<b>-0.380</b>
	Mixed	<b>-0.840</b>	<b>-0.652</b>	<b>-0.198</b>
	Pasture	<b>-0.758</b>	<b>-0.287</b>	<b>-0.143</b>
	Crops	<b>-0.717</b>	<b>0.270</b>	<b>-0.295</b>
Middle	Deciduous	<b>-0.835</b>	<b>-0.087</b>	<b>-0.698</b>
	Grassland	<b>-0.748</b>	<b>0.027</b>	<b>-0.155</b>
	Pasture	<b>-0.736</b>	<b>0.191</b>	<b>-0.520</b>
	Crops	<b>-0.589</b>	<b>-0.036</b>	<b>0.010</b>
Mountain	Evergreen	<b>-0.341</b>	<b>0.160</b>	<b>0.049</b>
	Shrub	<b>-0.212</b>	<b>0.384</b>	<b>0.186</b>
	Grass	<b>-0.008</b>	<b>0.159</b>	<b>0.049</b>
	Crops	<b>-0.107</b>	<b>0.384</b>	<b>-0.171</b>
Pacific	Evergreen	<b>-0.063</b>	<b>-0.442</b>	<b>-0.037</b>
	Shrub	<b>0.146</b>	<b>-0.268</b>	<b>-0.152</b>

Multiple linear regression models are also fitted for each vegetation cover. Stronger linear relationships result when different vegetation types are treated respectively. Coefficients of the regression models confirm visually determined GEI spatial patterns (Table 5).

**Table 5: Multiple linear regression models of GEI  
with geographic locations by vegetation types  
(P<0.001 for all cases)**

Regions	GEI	R <sup>2</sup>	Coefficients		
			Latitude	Longitude	Altitude
East	Deciduous	0.673	<b>-5.237</b>	<b>0.367</b>	<b>-0.008</b>
	Evergreen	0.746	<b>-5.415</b>	<b>0.754</b>	<b>-0.007</b>
	Mixed	0.717	<b>-4.412</b>	<b>0.500</b>	<b>0.004</b>
	Pasture	0.634	<b>-4.981</b>	<b>1.066</b>	<b>-0.012</b>
	Crops	0.641	<b>-4.207</b>	<b>1.320</b>	<b>-0.030</b>
Middle	Deciduous	0.716	<b>-2.519</b>	<b>-0.616</b>	<b>-0.031</b>
	Grassland	0.601	<b>-3.445</b>	<b>-2.651</b>	<b>-0.015</b>
	Pasture	0.563	<b>-1.959</b>	<b>-0.725</b>	<b>-0.012</b>
	Crops	0.369	<b>-3.096</b>	<b>-1.171</b>	<b>-0.012</b>
Mountain	Evergreen	0.119	<b>-0.449</b>	<b>-0.032</b>	<b>-0.000</b>
	Shrub	0.176	<b>-0.745</b>	<b>0.814</b>	<b>-0.000</b>
	Grass	0.036	<b>0.167</b>	<b>0.352</b>	<b>0.002</b>
	Crops	0.211	<b>-1.727</b>	<b>0.933</b>	<b>-0.004</b>
Pacific	Evergreen	0.304	<b>-2.274</b>	<b>-7.909</b>	<b>-0.006</b>
	Shrub	0.098	<b>-0.703</b>	<b>-3.606</b>	<b>-0.006</b>

### 4.3 Trend analysis of GEI multi-temporal imageries

GEI hypothetically should respond to phenotypic variability of vegetation types caused by climatic change. One prospective crucial application of GEI is to detect the inherent changes within ecosystems impacted by global warming through time. The 13-year GEI data are tested to assess their capability to reveal inherent land cover energy consumption pattern changes, caused by organism plastic modification, urbanization, and even species range shift. GEI for selected natural vegetation cover types in the East & Middle, Mountain and Pacific US are spatially averaged across the specific regions. Time series of GEI are compared by calculating departures from normals (Figures 4-6).

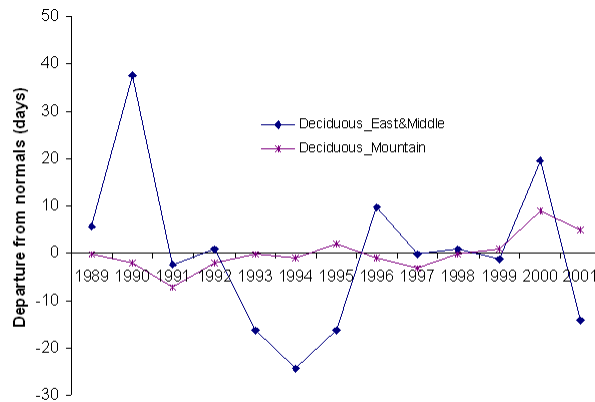


Figure 4: GEI departure from normals for deciduous forests.

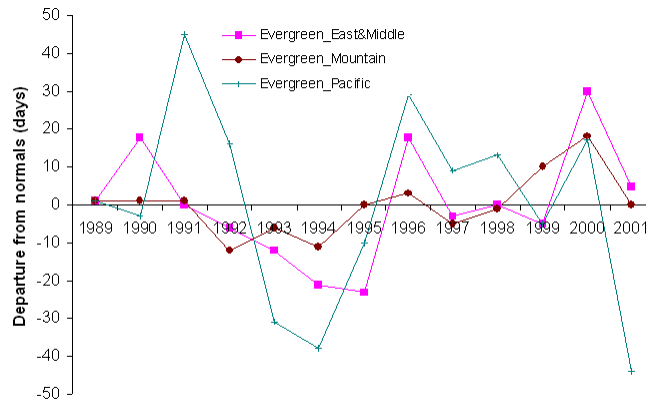
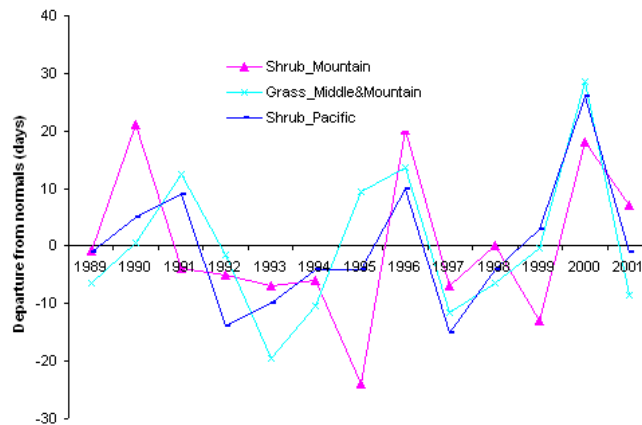


Figure 5: GEI departure from normals for evergreen forests.



**Figure 6: GEI departure from normals for shrub and grass.**

No obvious trends (that would indicate coherent internal vegetation cover change, as measured by GEI) were found for the time period under study (1989-2001). Potentially, the positive anomaly corresponds to changes within ecosystems that are hypothetically related to climatic warming. This is because of the less efficient utilization of energy by native plants (GEI increases) and possible northward invasion of high GEI characterized plants. Cooler temperatures are likely to encourage more efficient energy utilization (GEI decreases), which is related to the negative anomaly. We speculate that plastic response and adaptation of vegetation are sensitive to climatic variations over time as well as across the space.

## 5. Conclusions

The derived GEI monitors the acclimated strategies of plants to utilize spring energy for subsistence. Spatial variation of this new phenological metric shows clear correspondence with local climates, indicating the results of adaptation over time. It provides a strong indication of the adaptive nature of native species in varying climates. Boundaries of conventional vegetation cover types disappear and are merged into a new land cover characterization system using GEI. The new information available from GEI should prove useful for climatic impact assessment.

GEI can be used to assess energy consumption variability of the land surface over time. Although the current dataset does not suggest noticeable multiple-year change trends, the GEI approach is ready to be applied to newer time series datasets for tracking future changes. We assume the GEI method is sensitive enough to detect potential changes even before actual range shifts occur. Thus, inherent energy consumption pattern changes should be detected by GEI before actual species migrations are observed. This study is a first experiment combining satellite phenology and modeled phenology for monitoring the biospheric response to climate change at the continental scale, in order to specifically measure inherent energy consumption variation, which may be a major indicator of change due to global warming. This proposed GEI, and others using the same principle, but incorporating different remote-sensing SOS and climate-driven phenology models, should be widely developed and tested for applications in integrated phenological/ecosystem monitoring studies.

## References

- Badeck, F.W., Bondeau, A., Bottcher, K., Doktor, D., Lucht, W., Schaber, J., & Sitch, S. (2004). Responses of spring phenology to climate change. *New Phytologist*, 162, 295-309
- Barbour, M.G., Burk, J.H., & Pitts, W.D. (1987). *Terrestrial plant ecology*. Menlo Park, California: The Benjamin/Cummings
- Box, E.O. (1996). Plant functional types and climate at the global scale. *Journal of Vegetation Science*, 7, 309-320
- Budyko, M.I. (1974). *Climate and Life*. New York: Academic Press
- Christopherson, R.W. (2006). *Geosystems: An Introduction to Physical Geography*. Upper Saddle River, N.J.: Pearson Prentice Hall
- Cleland, E.E., Chuine, I., Menzel, A., Mooney, H.A., & Schwartz, M.D. (2007). Shifting plant phenology in response to global change. *Trends in Ecology & Evolution*, 22, 357-365

- de Beurs, K.M., & Henebry, G.M. (2005). Land surface phenology and temperature variation in the International Geosphere-Biosphere Program high-latitude transects. *Global Change Biology*, 11, 779-790
- Diaz, S., & Cabido, M. (1997). Plant functional types and ecosystem function in relation to global change. *Journal of Vegetation Science*, 8, 463-474
- Eidenshink, J. (1992). The 1990 conterminous U. S. AVHRR data set. *Photogrammetric Engineering and Remote Sensing*, 58, 809-813
- Fischer, A. (1994). A model for the seasonal variations of vegetation indices in coarse resolution data and its inversion to extract crop parameters. *Remote Sensing of Environment*, 48, 220-230
- Fisher, J.I., Mustard, J.F., & Vadeboncoeur, M.A. (2006). Green leaf phenology at Landsat resolution: Scaling from the field to the satellite. *Remote Sensing of Environment*, 100, 265-279
- Goward, S.N., Tucker, C.J., & Dye, D.G. (1985). North American vegetation patterns observed with the NOAA-7 advanced very high resolution radiometer. *Vegetatio(The Hague)*, 64, 3-14
- Homer, C., Huang, C., Yang, L., Wylie, B., & Coan, M. (2004). Development of a 2001 National Land-Cover Database for the United States. *Photogrammetric Engineering and Remote Sensing*, 70, 829-840
- Hopkins, A.D. (1938). *Bioclimatics: A Science of Life and Climate Relations*. Washington DC: United States Government Printing Office
- Huete, A., Didan, K., Miura, T., Rodriguez, E. P., Gao, X., & Ferreira, L. (2002). Overview of the radiometric and biophysical performance of the MODIS vegetation indices. *Remote Sensing of Environment*, 83, 195-213.
- Huntley, B. (1991). How Plants Respond to Climate Change: Migration Rates, Individualism and the Consequences for Plant Communities. *Annals of Botany*, 67, 15-22
- Jensen, J.R. (2000). *Remote Sensing of the Environment: An Earth Resource Perspective*. Upper Saddle River, NJ: Prentice Hall
- Justice, C.O., Vermote, E., Townshend, J.R.G., Defries, R., Roy, D.P., Hall, D.K., Salomonson, V.V., Privette, J.L., Riggs, G., & Strahler, A. (1998). The Moderate Resolution Imaging Spectroradiometer (MODIS): Land Remote Sensing for Global Change Research. *IEEE Transactions on Geoscience and Remote Sensing*, 36, 1228-1249
- Justice, C.O.T., J. R. G.; Holben, B. N.; & Tucker, C. J. (1985). Analysis of the phenology of global vegetation using meteorological satellite data. *International Journal of Remote Sensing*, 6, 1271-1318
- Leopold, A.C. (1951). Photoperiodism in Plants. *The Quarterly Review of Biology*, 26, 247-263

- Lloyd, D. (1990). A phenological classification of terrestrial vegetation cover using shortwave vegetation index imagery. *International Journal of Remote Sensing*, *11*, 2269-2279
- Malcolm, J.R., Markham, A., Neilson, R.P., & Caraci, M. (2002). Estimated migration rates under scenarios of global climate change. *Journal of Biogeography*, *29*, 835-849
- Markon, C.J., Fleming, M.D., & Binnian, E.F. (1995). Characteristics of vegetation phenology over the Alaskan landscape using AVHRR time-series data. *Polar Record*, *31*, 179-190
- Menzel, A., Sparks, T.H., Estrella, N., Koch, E., Aasa, A., Ahas, R., Alm-Kubler, K., Bissolli, P., Braslavska, O., Briede, A., Chmielewski, F.M., Crepinsek, Z., Curnel, Y., Dahl, A., Defila, C., Donnelly, A., Filella, Y., Jatcza, K., Mage, F., Mestre, A., Nordli, O., Penuelas, J., Pirinen, P., Remisova, V., Scheifinger, H., Striz, M., Susnik, A., Van Vliet, A.J.H., Wielgolaski, F.E., Zach, S., & Züst, A. (2006). European phenological response to climate change matches the warming pattern. *Global Change Biology*, *12*, 1969-1976
- Miller, D.H. (1981). *Energy at the Surface of the Earth: An Introduction to the Energetics of Ecosystems*. New York: Academic Press
- Monteith, J.L. (1975). *Vegetation and the atmosphere. Vol. 2, Case studies*. London: Academic Press
- Moulin, S., Kergoat, L., Viovy, N., & Dedieu, G. (1997). Global-scale assessment of vegetation phenology using NOAA/AVHRR satellite measurements. *Journal of Climate*, *10*, 1154-1170
- Overpeck, J.T., Bartlein, P.J., & Webb III, T. (1991). Potential Magnitude of Future Vegetation Change in Eastern North America: Comparisons with the Past. *Science*, *254*, 692
- Peñelas, J., & Boada, M. (2003). A global change-induced biome shift in the Montseny mountains (NE Spain). *Global Change Biology*, *9*, 131-140
- Potvin, C., & Tousignant, D. (1996). Evolutionary consequences of simulated global change: genetic adaptation or adaptive phenotypic plasticity. *Oecologia*, *108*, 683-693
- Prentice, I.C., Cramer, W., Harrison, S.P., Leemans, R., Monserud, R.A., & Solomon, A.M. (1992). Special Paper: A Global Biome Model Based on Plant Physiology and Dominance, Soil Properties and Climate. *Journal of Biogeography*, *19*, 117-134
- Reed, B.C., Brown, J.F., Vanderzee, D., Loveland, T.R., Merchant, J.W., & Ohlen, D.O. (1994). Measuring Phenological Variability from Satellite Imagery. *Journal of Vegetation Science*, *5*, 703-714
- Rosenberg, N.J. (1983). *Microclimate: The Biological Environment*. New York: Wiley-Interscience

- Rouse Jr, J.W., Haas, R.H., Schell, J.A., & Deering, D.W. (1974). Monitoring Vegetation Systems in the Great Plains with ERTS. *Third Earth Resources Technology Satellite-1 Symposium, Volume I: Technical Presentations*, 310-317
- Schaber, J. (2002). Phenology in Germany in the 20th Century Methods, Analyses and Models. Thesis, University of Potsdam, Germany
- Schwartz, M.D. (1994). Monitoring Global Change with Phenology - the Case of the Spring Green Wave. *International Journal of Biometeorology*, 38, 18-22
- Schwartz, M.D. (1997). Spring Index Models: An Approach to Connecting Satellite and Surface Phenology. In H.a.S. Lieth, M. D. (Ed.), *Phenology of Seasonal Climates I* (pp. 23-38). Netherlands: Backhuys Publishers
- Schwartz, M.D. (1998). Green-wave phenology. *Nature*, 394, 839-840
- Schwartz, M.D., Ahas, R., & Aasa, A. (2006). Onset of spring starting earlier across the Northern Hemisphere. *Global Change Biology*, 12, 343-351
- Schwartz, M.D., & Reed, B.C. (1999). Surface phenology and satellite sensor-derived onset of greenness: an initial comparison. *International Journal of Remote Sensing*, 20, 3451-3457
- Schwartz, M.D., Reed, B.C., & White, M.A. (2002). Assessing satellite-derived start-of-season measures in the conterminous USA. *International Journal of Climatology*, 22, 1793-1805
- Tarpley, J.D. (1991). The NOAA Global Vegetation Index product-A review. *Palaeogeography, Palaeoclimatology, Palaeoecology*, 90, 189-194
- White, M.A., Thornton, P.E., & Running, S.W. (1997). A continental phenology model for monitoring vegetation responses to interannual climatic variability. *Global Biogeochemical Cycles*, 11, 217-234
- Woodward, F.I. (1987). *Climate and Plant Distribution*. Cambridge: Cambridge University Press
- Zhang, X.Y., Friedl, M.A., & Schaaf, C.B. (2006). Global vegetation phenology from Moderate Resolution Imaging Spectroradiometer (MODIS): Evaluation of global patterns and comparison with in situ measurements. *Journal of Geophysical Research-Biogeosciences*, 111, G04017
- Zhang, X.Y., Friedl, M.A., Schaaf, C.B., Strahler, A.H., Hodges, J.C.F., Gao, F., Reed, B.C., & Huete, A. (2003). Monitoring vegetation phenology using MODIS. *Remote Sensing of Environment*, 84, 471-475
- Zhu, K. (1980). *Phenology (in Chinese)*. Beijing: Science Press